

**APATITE AND MERRILLITE FROM MARTIAN METEORITE NWA 7034.** A. R. Santos<sup>1</sup>, C. B. Agee<sup>1</sup>, F. M. McCubbin<sup>1</sup>, C. K. Shearer<sup>1</sup>, P. V. Burger<sup>1</sup>, Z. D. Sharp<sup>1</sup>, and M. Zimmer<sup>2</sup>, <sup>1</sup>Institute of Meteoritics, University of New Mexico, Albuquerque, NM 87131, <sup>2</sup>Los Alamos National Laboratory, Los Alamos, NM 87545 (asantos5@unm.edu).

**Introduction:** The martian meteorite NWA 7034 has been described by [1] as a volcanic monomict breccia. This meteorite has been determined to be water rich compared to previously known martian meteorites, and based on the amount of water released on stepped heating and on oxygen isotope data, the majority of this water originated on Mars [1]. This water is thought to be housed in different phases within the meteorite (e.g. apatite, hydrous oxides), and due to the unique nature of this meteorite it is important to understand these phases and determine what other petrologic information they can provide concerning the origin of this meteorite. The mineral apatite has proven to be a useful tool for investigating both magmatic volatiles and alteration fluids on several solar system bodies, including the Moon and Mars (e.g. [2, 3]), and thus is the focus of this study. We will use textural and geochemical data from different apatites to determine more about their formation conditions and melt volatiles.

**Methods:** Apatite from multiple sections of NWA 7034 was analyzed using the JEOL 8200 electron microprobe at UNM. Major elements were determined with EPMA, and select grains were then analyzed for rare earth elements with the Cameca IMS 4f ion microprobe (SIMS) also at UNM. Hydroxyl components have not been determined for apatites in NWA 7034, but they were estimated from EPMA analyses of F and Cl based on stoichiometry by assuming 1-F-Cl=OH. SIMS analyses of other martian apatites have shown this assumption to be a fairly safe one [3-5].

As this meteorite is a breccia, there are apatite grains present in both lithologic clasts and as individual mineral grains within the matrix. Apatites were classified as matrix apatite or clast apatite depending on their textural location in the sample. [6] defines three lithologic clast types found in this meteorite and provides further description of them. The two clast types that contain apatite are the gabbroic clasts and phosphate clasts.

**Results:** Apatite within the phosphate clasts are generally larger than gabbroic clast phosphates and occur as subhedral elongate grains with high aspect ratios. Apatite within the gabbroic clasts is typically subhedral to anhedral and occurs as grains adjacent to pyroxene and feldspar. Matrix apatites are sub- to euhedral in shape, some showing evidence of exsolved

REE phases. One apatite grain with a merrillite core was discovered (Figure 1), providing evidence for some secondary formation of apatite.

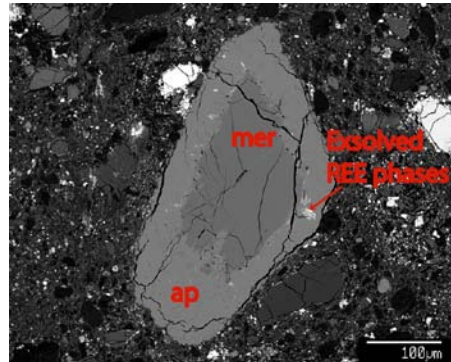


Figure 1: Merrillite (mer) core is surrounded by a secondary apatite (ap) rim. Note the rough boundary of the merrillite grain and the exsolved REE phases in the apatite.

The EPMA data show trace amounts of Na, Fe, Mg, and Ce in all apatites analyzed, with higher amounts of Mg, Na, and Ce in the merrillite grain. The apatite X-site is filled by Cl, F, and presumably OH. These quantities are plotted in the relative volatile abundance (RVA) diagram (Figure 2) from [7]. This diagram is used to determine the relative abundance of these three X-site occupants in the melt from which the apatite formed. The use of this diagram assumes apatite crystallized from a basaltic melt, which is certain for the clast apatites, but may not be true for all matrix apatites. Based on the data so far, gabbroic clast apatites formed from a melt with more water than chlorine and more chlorine than fluorine. The phosphate clast apatite originates from a melt with very similar relative abundances of volatiles. The matrix apatites are distributed across both of these fields as well. There are no fully distinct apatite populations based on X-site components, but some of the gabbroic clast apatite does plot closer to the F apex than any other apatites in NWA 7034.

Figure 3 shows REE data for select matrix apatite grains, two apatite grains from a phosphate clast, and the merrillite core. The merrillite has the highest REE abundance of any of the analyzed grains, including the apatite surrounding it (P1). The remaining matrix apatite has similar REE patterns but with slightly higher abundances than the whole rock value reported

in [1]. The apatite from the phosphate clast has slightly lower REE abundances than the whole rock and matrix apatites. The clast apatites also have a small positive Eu anomaly, unlike all other analyzed apatites.

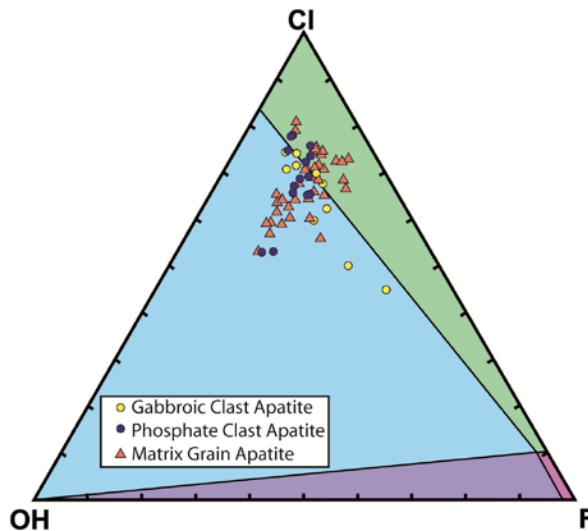


Figure 2: Relative volatile abundance (RVA) diagram of apatite from the matrix and two clast types. OH was calculated using EPMA data and assuming  $1-F-Cl=OH$ . Different colored fields represent different relative abundances of F, Cl, and  $H_2O$  in the basaltic melt the apatites crystallized from. Green: melt  $Cl > H_2O > F$ , blue: melt  $H_2O > Cl > F$ , light purple: melt  $H_2O > F > Cl$ , dark purple: melt  $F > Cl, H_2O$ . Matrix grain data is from [1].

**Interpretations:** The RVA diagram (Fig. 2) shows evidence for apatites formed by melts whose volatile content was dominated by  $H_2O$  and Cl. The gabbroic clast apatite is mostly restricted to the water dominated field, but is close to the Cl dominated field while the phosphate clast has apatite that plot in both fields. The spread of phosphate clast apatite across this boundary suggests some phosphate clasts formed from either separate melts or the same melt after a change in the dominant volatile occurred. The matrix apatite shows a similar spread in X-site component as the phosphate clast apatite, but the phosphate clast apatite is distinct from matrix apatite based on REE data. The positive Eu anomaly in the phosphate clast apatite may prove to be a distinguishing feature for phosphate clasts, but more data is needed to be certain.

The positive Eu anomaly in the phosphate clast apatite could be a result of a source region process (e.g. residual clinopyroxene in the source region excluding Eu [8]). A negative Eu anomaly is observed in apatite from the matrix, suggesting different sources or parent magmas for the two textural populations of apatite analyzed in NWA 7034. Analyses of REE's in apatite

from the gabbroic clast population [6] have not yet been conducted, but analyses are ongoing.

The merrillite grain surrounded by apatite in the matrix (Fig. 1) is textural evidence for secondary apatite formation in this meteorite by fluid processes [9]. The uneven boundaries of the merrillite grain, variation in REE abundances in the surrounding apatite, and higher REE abundance in the merrillite all point to the apatite being formed by a reaction between merrillite and a fluid. Additional work is required to characterize the nature and timing of the metasomatic event that formed this apatite and how it relates to other apatites in the breccia matrix, and that work is ongoing. Furthermore, we are currently measuring stable isotopes (Cl, H/D, O) in individual phosphate grains using the Cameca IMS 1280 ion microprobe lab at Los Alamos National Laboratory.

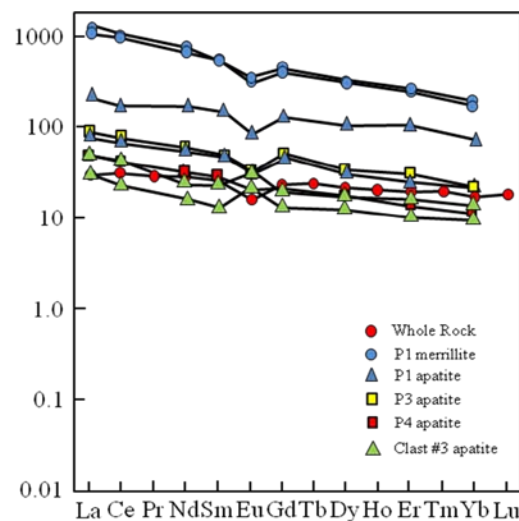


Figure 3: REE abundances of phosphate phases in NWA 7034 normalized to Cl from [10]. Analyses P1-4 refer to matrix apatite grains and the analyses from Clast #3 are from a phosphate clast.

**References:** [1] Agee C. B. et al. (2013) *Scienceexpress*, 10.1126/science.1228858. [2] McCubbin F. M. et al. (2010) *PNAS*, 107, 11223-11228. [3] McCubbin F. M. et al. (2012) *Geology*, 40, 683-686. [4] Greenwood J. P. et al. (2008) *GRL*, 35, L05203. [5] Boctor, N. A. et al. (2003) *GCA*, 67, 3971-3989. [6] Santos A. R. et al. (2013a) *LPSC XLIV*. [7] McCubbin F. M. et al. (2013) *MAPS In Press*. [8] Cox K. G., Bell J. D., and Pankhurst R. J. (1979) *Interp. of Ig. Rocks*. [9] Shearer C. K. et al. (2011) *MAPS*, 46, 1345-1362. [10] Anders E. and Grevesse N. (1989) *GCA*, 53, 197-214.